Biomedical Optics EXPRESS

In vivo multiplexed molecular imaging of esophageal cancer via spectral endoscopy of topically applied SERS nanoparticles

Yu Winston Wang,[1] Soyoung Kang,[1] Altaz Khan,[2] Philip Q. Bao,[3] and Jonathan T.C. Liu[1,*]

[1]*Department of Mechanical Engineering, University of Washington, Seattle, WA 98195, USA*
[2]*Department of Biomedical Engineering, Stony Brook University (SUNY), Stony Brook, NY 11794, USA*
[3]*Department of Surgery, Stony Brook Medicine, Stony Brook, NY 11794, USA*
[*]*jonliu@uw.edu*

Abstract: The biological investigation and detection of esophageal cancers could be facilitated with an endoscopic technology to screen for the molecular changes that precede and accompany the onset of cancer. Surface-enhanced Raman scattering (SERS) nanoparticles (NPs) have the potential to improve cancer detection and investigation through the sensitive and multiplexed detection of cell-surface biomarkers. Here, we demonstrate that the topical application and endoscopic imaging of a multiplexed cocktail of receptor-targeted SERS NPs enables the rapid detection of tumors in an orthotopic rat model of esophageal cancer. Antibody-conjugated SERS NPs were topically applied on the lumenal surface of the rat esophagus to target EGFR and HER2, and a miniature spectral endoscope featuring rotational scanning and axial pull-back was employed to comprehensively image the NPs bound on the lumen of the esophagus. Ratiometric analyses of specific vs. nonspecific binding enabled the visualization of tumor locations and the quantification of biomarker expression in agreement with immunohistochemistry and flow cytometry validation data.

OCIS codes: (170.5660) Raman spectroscopy; (170.2150) Endoscopic imaging; (110.2350) Fiber optics imaging; (170.0170) Medical optics and biotechnology; (170.2680) Gastrointestinal; (160.4236) Nanomaterials.

References and links

1. D. M. Parkin, F. I. Bray, and S. S. Devesa, "Cancer burden in the year 2000. The global picture," Eur. J. Cancer **37**(Suppl 8), S4–S66 (2001).
2. R. F. Souza, "Molecular and biologic basis of upper gastrointestinal malignancy--esophageal carcinoma," Surg. Oncol. Clin. N. Am. **11**(2), 257–272 (2002).
3. J. C. Layke and P. P. Lopez, "Esophageal cancer: a review and update," Am. Fam. Physician **73**(12), 2187–2194 (2006).
4. A. P. Polednak, "Trends in survival for both histologic types of esophageal cancer in US surveillance, epidemiology and end results areas," Int. J. Cancer **105**(1), 98–100 (2003).
5. M. Younes, D. E. Henson, A. Ertan, and C. C. Miller, "Incidence and survival trends of esophageal carcinoma in the United States: racial and gender differences by histological type," Scand. J. Gastroenterol. **37**(12), 1359–1365 (2002).
6. M. B. Sturm, B. P. Joshi, S. Lu, C. Piraka, S. Khondee, B. J. Elmunzer, R. S. Kwon, D. G. Beer, H. D. Appelman, D. K. Turgeon, and T. D. Wang, "Targeted imaging of esophageal neoplasia with a fluorescently labeled peptide: first-in-human results," Sci. Transl. Med. **5**(184), 184ra61 (2013).
7. E. L. Bird-Lieberman, A. A. Neves, P. Lao-Sirieix, M. O'Donovan, M. Novelli, L. B. Lovat, W. S. Eng, L. K. Mahal, K. M. Brindle, and R. C. Fitzgerald, "Molecular imaging using fluorescent lectins permits rapid endoscopic identification of dysplasia in Barrett's esophagus," Nat. Med. **18**(2), 315–321 (2012).
8. T. I. Samoylova, N. E. Morrison, L. P. Globa, and N. R. Cox, "Peptide phage display: opportunities for development of personalized anti-cancer strategies," Anticancer. Agents Med. Chem. **6**(1), 9–17 (2006).

#245684 Received 10 Jul 2015; revised 10 Aug 2015; accepted 24 Aug 2015; published 1 Sep 2015

9. R. Weissleder, B. D. Ross, A. Rehemtulla, and S. S. Gambhir, *Molecular Imaging: Principles and Practice* (People's Medical Publishing House, 2010).
10. A. Hellebust and R. Richards-Kortum, "Advances in molecular imaging: targeted optical contrast agents for cancer diagnostics," Nanomedicine (Lond.) **7**(3), 429–445 (2012).
11. Q. T. Nguyen and R. Y. Tsien, "Fluorescence-guided surgery with live molecular navigation--a new cutting edge," Nat. Rev. Cancer **13**(9), 653–662 (2013).
12. Y. Wang, B. Yan, and L. Chen, "SERS Tags: Novel Optical Nanoprobes for Bioanalysis," Chem. Rev. **113**(3), 1391–1428 (2013).
13. C. L. Zavaleta, B. R. Smith, I. Walton, W. Doering, G. Davis, B. Shojaei, M. J. Natan, and S. S. Gambhir, "Multiplexed imaging of surface enhanced Raman scattering nanotags in living mice using noninvasive Raman spectroscopy," Proc. Natl. Acad. Sci. U.S.A. **106**(32), 13511–13516 (2009).
14. C. L. Zavaleta, E. Garai, J. T. C. Liu, S. Sensarn, M. J. Mandella, D. Van de Sompel, S. Friedland, J. Van Dam, C. H. Contag, and S. S. Gambhir, "A Raman-based endoscopic strategy for multiplexed molecular imaging," Proc. Natl. Acad. Sci. U.S.A. **110**(25), E2288–E2297 (2013).
15. S. E. Bohndiek, A. Wagadarikar, C. L. Zavaleta, D. Van de Sompel, E. Garai, J. V. Jokerst, S. Yazdanfar, and S. S. Gambhir, "A small animal Raman instrument for rapid, wide-area, spectroscopic imaging," Proc. Natl. Acad. Sci. U.S.A. **110**(30), 12408–12413 (2013).
16. P. Z. McVeigh, R. J. Mallia, I. Veilleux, and B. C. Wilson, "Widefield quantitative multiplex surface enhanced Raman scattering imaging in vivo," J. Biomed. Opt. **18**(4), 046011 (2013).
17. E. Garai, S. Sensarn, C. L. Zavaleta, D. Van de Sompel, N. O. Loewke, M. J. Mandella, S. S. Gambhir, and C. H. Contag, "High-sensitivity, real-time, ratiometric imaging of surface-enhanced Raman scattering nanoparticles with a clinically translatable Raman endoscope device," J. Biomed. Opt. **18**(9), 096008 (2013).
18. R. J. Mallia, P. Z. McVeigh, I. Veilleux, and B. C. Wilson, "Filter-based method for background removal in high-sensitivity wide-field-surface-enhanced Raman scattering imaging in vivo," J. Biomed. Opt. **17**(7), 0760171 (2012).
19. J. V. Jokerst, Z. Miao, C. Zavaleta, Z. Cheng, and S. S. Gambhir, "Affibody-Functionalized Gold-Silica Nanoparticles for Raman Molecular Imaging of the Epidermal Growth Factor Receptor," Small **7**(5), 625–633 (2011).
20. X. Wang, X. Qian, J. J. Beitler, Z. G. Chen, F. R. Khuri, M. M. Lewis, H. J. C. Shin, S. Nie, and D. M. Shin, "Detection of circulating tumor cells in human peripheral blood using surface-enhanced Raman scattering nanoparticles," Cancer Res. **71**(5), 1526–1532 (2011).
21. S. Lee, H. Chon, S.-Y. Yoon, E. K. Lee, S.-I. Chang, D. W. Lim, and J. Choo, "Fabrication of SERS-fluorescence dual modal nanoprobes and application to multiplex cancer cell imaging," Nanoscale **4**(1), 124–129 (2012).
22. L. Sun, K.-B. Sung, C. Dentinger, B. Lutz, L. Nguyen, J. Zhang, H. Qin, M. Yamakawa, M. Cao, Y. Lu, A. J. Chmura, J. Zhu, X. Su, A. A. Berlin, S. Chan, and B. Knudsen, "Composite organic-inorganic nanoparticles as Raman labels for tissue analysis," Nano Lett. **7**(2), 351–356 (2007).
23. X. Su, J. Zhang, L. Sun, T. W. Koo, S. Chan, N. Sundararajan, M. Yamakawa, and A. A. Berlin, "Composite organic-inorganic nanoparticles (COINs) with chemically encoded optical signatures," Nano Lett. **5**(1), 49–54 (2005).
24. Y. W. Wang, A. Khan, M. Som, D. Wang, Y. Chen, S. Y. Leigh, D. Meza, P. Z. McVeigh, B. C. Wilson, and J. T. C. Liu, "Rapid ratiometric biomarker detection with topically applied SERS nanoparticles," Technology (Singap World Sci) **2**(2), 118–132 (2014).
25. A. S. Thakor, R. Luong, R. Paulmurugan, F. I. Lin, P. Kempen, C. Zavaleta, P. Chu, T. F. Massoud, R. Sinclair, and S. S. Gambhir, "The fate and toxicity of Raman-active silica-gold nanoparticles in mice," Sci. Transl. Med. **3**(79), 79ra33 (2011).
26. C. L. Zavaleta, K. B. Hartman, Z. Miao, M. L. James, P. Kempen, A. S. Thakor, C. H. Nielsen, R. Sinclair, Z. Cheng, and S. S. Gambhir, "Preclinical evaluation of Raman nanoparticle biodistribution for their potential use in clinical endoscopy imaging," Small **7**(15), 2232–2240 (2011).
27. Y. W. Wang, A. Khan, S. Y. Leigh, D. Wang, Y. Chen, D. Meza, and J. T. C. Liu, "Comprehensive spectral endoscopy of topically applied SERS nanoparticles in the rat esophagus," Biomed. Opt. Express **5**(9), 2883–2895 (2014).
28. K. M. Tichauer, K. S. Samkoe, K. J. Sexton, J. R. Gunn, T. Hasan, and B. W. Pogue, "Improved tumor contrast achieved by single time point dual-reporter fluorescence imaging," J. Biomed. Opt. **17**(6), 066001 (2012).
29. J. T. C. Liu, M. W. Helms, M. J. Mandella, J. M. Crawford, G. S. Kino, and C. H. Contag, "Quantifying Cell-Surface Biomarker Expression in Thick Tissues with Ratiometric Three-Dimensional Microscopy," Biophys. J. **96**(6), 2405–2414 (2009).
30. K. M. Tichauer, K. S. Samkoe, K. J. Sexton, S. K. Hextrum, H. H. Yang, W. S. Klubben, J. R. Gunn, T. Hasan, and B. W. Pogue, "In vivo quantification of tumor receptor binding potential with dual-reporter molecular imaging," Mol. Imaging Biol. **14**(5), 584–592 (2012).
31. W. E. Doering, M. E. Piotti, M. J. Natan, and R. G. Freeman, "SERS as a Foundation for Nanoscale, Optically Detected Biological Labels," Adv. Mater. **19**(20), 3100–3108 (2007).
32. M. M. Moasser, A. Basso, S. D. Averbuch, and N. Rosen, "The tyrosine kinase inhibitor ZD1839 ("Iressa") inhibits HER2-driven signaling and suppresses the growth of HER2-overexpressing tumor cells," Cancer Res. **61**(19), 7184–7188 (2001).

#245684 Received 10 Jul 2015; revised 10 Aug 2015; accepted 24 Aug 2015; published 1 Sep 2015

33. N. Gaborit, C. Larbouret, J. Vallaghe, F. Peyrusson, C. Bascoul-Mollevi, E. Crapez, D. Azria, T. Chardès, M.-A. Poul, G. Mathis, H. Bazin, and A. Pèlegrin, "Time-resolved fluorescence resonance energy transfer (TR-FRET) to analyze the disruption of EGFR/HER2 dimers: a new method to evaluate the efficiency of targeted therapy using monoclonal antibodies," J. Biol. Chem. **286**(13), 11337–11345 (2011).
34. M. Schmidt, N. E. Hynes, B. Groner, and W. Wels, "A bivalent single-chain antibody-toxin specific for ErbB-2 and the EGF receptor," Int. J. Cancer **65**(4), 538–546 (1996).
35. W. Wels, R. Beerli, P. Hellmann, M. Schmidt, B. M. Marte, E. S. Kornilova, A. Hekele, J. Mendelsohn, B. Groner, and N. E. Hynes, "EGF receptor and p185erbB-2-specific single-chain antibody toxins differ in their cell-killing activity on tumor cells expressing both receptor proteins," Int. J. Cancer **60**(1), 137–144 (1995).
36. B. Stea, R. Falsey, K. Kislin, J. Patel, H. Glanzberg, S. Carey, A. A. Ambrad, E. J. Meuillet, and J. D. Martinez, "Time and dose-dependent radiosensitization of the glioblastoma multiforme U251 cells by the EGF receptor tyrosine kinase inhibitor ZD1839 ('Iressa')," Cancer Lett. **202**(1), 43–51 (2003).
37. A. A. Habib, S. J. Chun, B. G. Neel, and T. Vartanian, "Increased Expression of Epidermal Growth Factor Receptor Induces Sequestration of Extracellular Signal-Related Kinases and Selective Attenuation of Specific Epidermal Growth Factor-Mediated Signal Transduction Pathways," Mol. Cancer Res. **1**(3), 219–233 (2003).
38. S. Y. Leigh, M. Som, and J. T. C. Liu, "Method for Assessing the Reliability of Molecular Diagnostics Based on Multiplexed SERS-Coded Nanoparticles," PLoS One **8**(4), e62084 (2013).
39. B. D. Chithrani, A. A. Ghazani, and W. C. W. Chan, "Determining the Size and Shape Dependence of Gold Nanoparticle Uptake into Mammalian Cells," Nano Lett. **6**(4), 662–668 (2006).
40. S. Keren, C. Zavaleta, Z. Cheng, A. de la Zerda, O. Gheysens, and S. S. Gambhir, "Noninvasive molecular imaging of small living subjects using Raman spectroscopy," Proc. Natl. Acad. Sci. U.S.A. **105**(15), 5844–5849 (2008).
41. E. Garai, S. Sensarn, C. L. Zavaleta, N. O. Loewke, S. Rogalla, M. J. Mandella, S. A. Felt, S. Friedland, J. T. C. Liu, S. S. Gambhir, and C. H. Contag, "A Real-Time Clinical Endoscopic System for Intraluminal, Multiplexed Imaging of Surface-Enhanced Raman Scattering Nanoparticles," PLoS One **10**(4), e0123185 (2015).

1. Introduction

Esophageal cancer causes approximately one-sixth of all cancer-related deaths worldwide [1, 2]. Esophageal cancer patients often present with advanced metastatic disease at the time of diagnosis [3], resulting in poor survival and cure rates [4, 5]. One promising means of improving the early detection and biological investigation of esophageal cancer is to screen for the molecular changes that precede and accompany the onset of cancer [6, 7]. Since esophageal cancer arises from the epithelial cells located at the lumenal surface of the esophagus, the cell-surface and tissue biomarkers at the lumenal surface could be imaged to monitor disease progression. However, due to the fact that biomarker expression profiles vary greatly between patients and within individuals over time [8], accurate disease diagnosis, patient stratification, and biological investigation requires the assessment of a large number of molecular targets.

Over the past few decades, various types of exogenous contrast agents have been developed for the molecular imaging of fresh tissues *ex vivo* and *in vivo* [9–11]. Among these contrast agents, surface-enhanced Raman-scattering (SERS) nanoparticles (NPs) have attracted interest for cancer imaging due to their excellent multiplexing capabilities [12]. The SERS NPs utilized in this study may be engineered as various "flavors," each of which generates a unique Raman spectral "fingerprint" when illuminated with a single laser at 785 nm. These diverse "barcode" or "fingerprint" spectra allow for the multiplexed detection of large panels of NPs when applied in live animals and human tissues [13–18]. Each flavor of SERS NPs can be conjugated to an antibody or small-molecule ligand to target a specific cell-surface or tissue biomarker [19–24]. After orally introducing a mixture of these biomarker-targeted NPs into the esophagus (e.g., by having the subject ingest a cocktail of NPs), physicians and tumor biologists may potentially be able to visualize the expression of a panel of molecular biomarkers during endoscopic procedures to accurately detect tumors and to study their progression over time. No toxicity effects have been observed, with negligible systemic uptake, when SERS NPs have been applied topically in the rectum of mice [25, 26]. However, SERS NPs are not yet approved for administration in the human esophagus. Therefore, our current work utilizes a rat model to demonstrate the feasibility of this endoscopic imaging approach for preclinical investigations. Major challenges such as FDA

#245684 Received 10 Jul 2015; revised 10 Aug 2015; accepted 24 Aug 2015; published 1 Sep 2015

approval and the improvement of imaging speeds must be addressed in order to translate this technique into clinical use.

We previously described a rotational spectral-imaging endoscope to image the rat esophagus in which preliminary validation was performed using untargeted SERS NPs and matrigel phantoms pre-loaded with SERS NPs [27]. In this article, we demonstrate (for the first time) the feasibility of *in vivo* multiplexed molecular endoscopy of biomarker-positive tumors in a rat esophagus using targeted SERS NPs that are topically applied into the lumen of the esophagus. Ratiometric imaging of targeted vs. untargeted SERS NPs provides a means of controlling for nonspecific effects such as uneven NP delivery, off-target binding, and variations in tissues permeability and retention [24, 28–30]. We show that this ratiometric quantification of specific vs. nonspecific binding is in agreement with both flow cytometry and immunohistochemistry validation data.

2. Methods

2.1 SERS NPs and functionalization

The SERS NPs used in this study were purchased from Cabot Security Materials Inc. These NPs have a sandwich structure, a 60-nm gold core, a unique layer of Raman reporter adsorbed onto the gold core surface, and an outer silica coating, totaling 120 nm in diameter [13, 31]. Three "flavors" of NPs were used here, identified as S420, S421 and S440, each of which emits a unique fingerprint Raman spectrum when illuminated with a laser at 785-nm. These spectral differences are due to chemical differences in the Raman reporter layer. To enable the imaging of cell-surface biomarker targets, the SERS NPs were functionalized with monoclonal antibodies (mAb) according to a previously described conjugation protocol [24]. In brief, the NPs were first labeled with a fluorophore (Cyto 647-maleimide from Cytodiagnostics Inc, part No. NF647-3-01) for flow-cytometry characterization, and then conjugated with either an anti-EGFR mAb (Thermo Scientific, MS-378-PABX), an anti-HER2 mAb (Thermo Scientific, MS-229-PABX), or an isotype control mAb (Thermo Scientific, MA110407) at 500 molar equivalents per NP.

The conjugated NPs were tested with four cell lines (purchased from ATCC) that express various levels of EGFR and HER2, including A431 (a human epidermoid carcinoma cell line that highly overexpresses EGFR and moderately expresses HER2), U251 (a human glioblastoma cell line that moderately expresses EGFR and HER2), SkBr3 (a human breast adenocarcinoma cell line that highly overexpresses HER2 and moderately expresses EGFR), and 3T3 (a normal mouse fibroblast cell line that expresses negligible amounts of EGFR and HER2 [32–37]. Flow-cytometry analyses demonstrate a high binding affinity of these conjugated NPs to their cell-surface receptor targets: either EGFR or HER2 (Fig. 1). The different binding levels of various NP conjugates to different cell lines may be quantified by calculating the geometric mean of the fluorescent intensities (MFI). The MFIs of negative-control 3T3 cells stained with the three NP conjugates (two targeted and one control) are similar. For EGFR-NPs, the binding level (MFI of EGFR-NPs vs. isotype-NPs) increases with the following order of cell lines: 3T3 < SkBr3 < U251 < A431. For the HER2-NPs, the binding level (MFI of HER2-NPs vs. isotype-NPs) increases with the following order of cell lines: 3T3 < U251 < A431 < SkBr3. These results are consistent with the known receptor expression levels of these cell lines [32–37].

2.2 Rat model of esophageal tumors

In preparation for the development of an orthotopic esophageal cancer model, subcutaneous tumor xenografts were first implanted into female nude mice (6-8 weeks, Charles River Laboratories, model NU(NCr)-Foxn1^{nu}). These tumor xenografts were later surgically implanted into the esophagus of Male Fischer 344 Inbred rats (7-9 weeks, Harlan Laboratories, Inc), which were used for esophageal-imaging studies. All animal work was

#245684 Received 10 Jul 2015; revised 10 Aug 2015; accepted 24 Aug 2015; published 1 Sep 2015

performed in accordance with guidelines approved by the Institutional Animal Care and Use Committee (IACUC) at Stony Brook University or the University of Washington.

To develop tumor xenografts, three human cancer cell lines that differ in EGFR and HER2 expression levels (see Section 2.1) – A431, U251 and SkBr3 – were suspended in matrigel (BD biosciences, 354234) in a 1:1 volume ratio to form a 100–200 μL mixture (1×10^6 A431 cells, 3×10^6 U251 cells or 5×10^6 SkBr3 cells per mixture). At 7-9 weeks of age, nude mice were subcutaneously implanted with the cell mixture at different sites on their flanks. A maximum of three sites were implanted on each mouse with a distance of 1–2 cm between adjacent sites. When the tumors reached a size of 8 to 10 mm (about 3–5 weeks), the mice were euthanized by CO_2 inhalation, followed by the surgical removal of the implanted tumors.

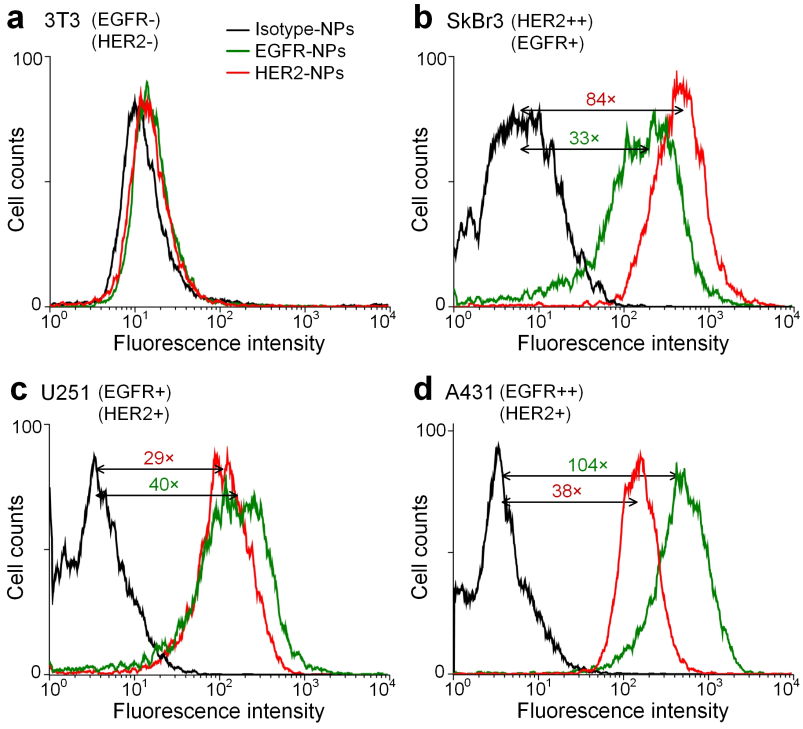

Fig. 1. Flow cytometry validation of conjugated NPs with various biomarker-positive cell lines. EGFR-NPs, HER2-NPs and isotype-NPs were individually used to stain (a) 3T3, (b) SkBr3, (c) U251 or (d) A431 cell lines. The colored numbers represent the ratio of the mean fluorescence intensity (MFI) between a targeted NP (EGRF-NP or HER2-NP) vs. an untargeted NP (isotype-NP).

An orthotopic rat esophageal model was developed for imaging studies. For *ex vivo* experiments, rats were euthanized via inhalation of CO_2, followed by the surgical removal of the esophagus (~8 cm in length). Several 3-mm diameter holes were cut in the wall of the esophagus (Fig. 2(a)). Small tumor explants, obtained from subcutaneous tumor xenografts in mice, were positioned on top of the holes in the esophagus wall, and glued into place with dermabond (a tissue adhesive). A 20-μL pipet tip was used to apply the dermabond between the tumor explants and the rat esophagus in order to form a tight seal (Fig. 2(b)) such that SERS NPs applied within the lumen of the esophagus would not leak out of the esophagus during staining procedures (Fig. 2(c)). For *in vivo* experiments, rats were anesthetized via intraperitoneal injection of ketamine and xylazine. A small incision was made through the neck skin, and the cervical muscles were separated. The cervical esophagus was carefully exposed, and a few 3-mm diameter holes were cut in the wall of the esophagus. Small tumor

#245684 Received 10 Jul 2015; revised 10 Aug 2015; accepted 24 Aug 2015; published 1 Sep 2015

explants, obtained from subcutaneous tumor xenografts in mice, were positioned on top of the holes in the esophagus wall, and glued into place with dermabond. The esophagus was stained via an oral gavage procedure and imaged immediately afterwards (*in vivo*). After the imaging studies were completed, the rats were euthanized via inhalation of CO_2.

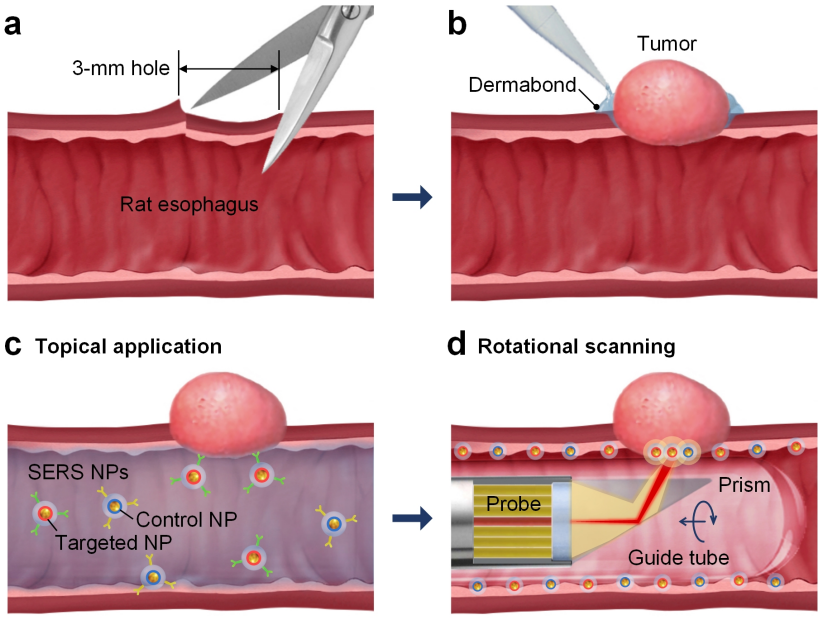

Fig. 2. Schematic of the development and endoscopic imaging of a rat esophageal tumor model. (a) and (b) show the construction of an orthotopic esophageal tumor model by surgically attaching a tumor xenograft that was previously implanted subcutaneously in the flank of a nude mouse. (c) Topical application of multiplexed SERS NPs on the lumenal surface of the esophagus for ratiometric biomarker detection. (d) Endoscopic imaging of the SERS NPs via rotational pull-back of a fiber-bundle-based imaging probe.

2.3 Spectral-imaging endoscopy of SERS NPs in the rat esophagus

For molecular endoscopy of the rat esophagus, a glass guide tube (OD 3.25 mm, ID 2.6 mm, Rayotek Scientific Inc) was first inserted into the rat esophagus, such that the lumen of the esophagus was wrapped tightly around the guide tube. A spectral-imaging probe (OD 2.5 mm, FiberTech Optica Inc.) was then inserted into the guide tube and was rotated and translated axially to comprehensively image the SERS NPs applied on the esophagus (Fig. 2(d)). This form of laser-scanned imaging is referred to here as "rotational pull-back imaging."

A multimode fiber (100-μm core, 0.10 NA) at the center of the imaging probe was used to illuminate the esophagus using a 785-nm diode laser (~15 mW at the tissue) while 27 multimode fibers (200-μm core, 0.22 NA) surrounding the illumination fiber were used to collect optical signals (Fig. 2(d)). A 30° prism (Tower Optical Inc.) was adhered to the tip of the fiber-bundle probe in order to deflect the laser beam onto the lumen of the esophagus. Based on the working distance between the illumination fiber and the lumen of the esophagus (4 mm), and the NA of the illumination fiber (0.1), a 0.5-mm diameter spot (FWHM) was illuminated at the lumen of the esophagus (Fig. 2(d)), which defines the spatial resolution of our device. A customized spectrometer (Andor Holospec) was used to disperse the light collected from the 27 collection fibers onto a cooled deep-depletion spectroscopic CCD (Andor Newton, DU920P-BR-DD) with a spectral resolution of ~2 nm (~30 cm^{-1}). The rigid imaging probe was held and rotated by a hollow-shaft stepper motor (Nanotec ST5918) that was translated axially with a linear stage (Zaber Technologies, T-LSM200A). The imaging probe was alternately rotated in the positive and negative directions (± 180 deg) to protect the

#245684 Received 10 Jul 2015; revised 10 Aug 2015; accepted 24 Aug 2015; published 1 Sep 2015

fiber bundles from twisting. A National Instruments data acquisition system programmed in LabVIEW was used to control the stepper motor and translation stage for laser-scanned imaging of the rat esophagus, as well as to demultiplex the acquired spectra and reconstruct images of the concentration and concentration ratio of various SERS NP flavors. Since the illumination spot size was 0.5 mm, in order to sample the esophagus at nearly the Nyquist sampling criterion, the imaging probe acquired 30 spectral acquisitions per rotation (a pixel pitch of 12° or 0.34 mm), and was translated by 0.3 mm in the axial direction during each rotation. For these studies, we utilized a spectral acquisition rate (pixel clock) of 10 spectra/sec (0.1 sec/pixel). Additional details about the system, the spectra demultiplexing algorithm, and the reproducibility and linearity of the spectral measurements, have been described previously [27, 38].

For *ex vivo* experiments, the esophagus was rinsed with PBS and then irrigated with a mucolytic agent (N-Acetyl-L-cysteine, or NAC for short, Sigma-Aldrich, part No. A7250, 0.5 mL at 0.1 g/mL, 30-sec rinse) to allow the NPs to access and adhere to the esophagus tissue more effectively. The esophagus was first imaged prior to being stained in order to measure the tissue background. Multiple spectra were acquired by performing rotational pull-back imaging of both normal esophagus and tumor areas. Multiple tissue background reference components were used for spectral demultiplexing analysis in order to account for slight differences in the spectral background of normal esophagus and tumor tissues. After acquiring tissue background spectra, a 0.1-mL mixture of EGFR-NP and isotype-NP (150 pM/flavor with an addition of 1% BSA) was pipetted into the lumen of the esophagus and allowed to incubate for a duration of 10 min, followed by a rapid PBS rinse (0.2 mL). The esophagus was imaged again to measure the NP concentrations for biomarker detection.

For *in vivo* experiments, rats were anesthetized and the 3.25-mm diameter guide tube was inserted into the rat's esophagus until gently opposed by the esophageal sphincter at the entrance to the stomach. The imaging probe was then inserted within the guide tube for rotational pull-back imaging (similar to *ex vivo* experiments).

Upon completion of all imaging experiments, esophagus tissues and tumor xenografts were fixed in 10% formalin and submitted for histopathology (IHC and H&E staining).

3. Results

3.1 Demonstration of endoscopic imaging ex vivo

Ex vivo experiments were first performed to test the ability to detect tumors (Figs. 3(a)–3(d)). The excised esophagus was implanted with 3 tumor xenografts (Fig. 3(b)) – U251, SkBr3 and A431 – each of which exhibits a different level of EGFR expression (Fig. 1). Endoscopic imaging was performed by scanning a 2.5-cm esophagus section (2500 acquisitions) with an integration time of 0.1 sec per spectrum (0.1 sec per image pixel).

The image of the measured concentrations and ratios are shown in Figs. 3(c) and 3(d). The image showing the distribution of EGFR-NPs fails to identify the three tumors due to the high variability in NP concentrations across the tissue (Fig. 3(c)). In comparison, the ratiometric image of targeted vs. untargeted SERS NPs (Fig. 3(d)) is insensitive to nonspecific variations in the absolute NP concentrations (due to uneven delivery and nonspecific accumulation) and accurately reveals the location of the tumors. In addition, as shown in Fig. 3(d) and 3(e), the ratiometric image of EGFR-NPs vs. isotype-NPs agrees qualitatively with the corresponding EGFR immunohistochemistry (IHC) images of the various tissues.

3.2 Demonstration of endoscopic imaging in vivo

In vivo experiments were performed to demonstrate the ability to simultaneously image the expression of multiple biomarkers through the oral administration of a mixture of three different flavors of SERS NPs (Fig. 4). An oral gavage catheter was placed within the rat esophagus to first deliver 0.2-mL of NAC (0.1 g/mL, 30 sec), which is a mucolytic agent, then

#245684 Received 10 Jul 2015; revised 10 Aug 2015; accepted 24 Aug 2015; published 1 Sep 2015

0.2-mL of PBS to rinse out the NAC (10 sec), and finally an equimolar mixture of EGFR-NPs, HER2-NPs, and isotype-NPs (150 pM/each, 0.12 mL). After 10 minutes, unbound NPs were rinsed away by irrigating the esophagus for 10 sec with 0.2-mL of PBS. Once the staining procedure was completed, we performed rotational pull-back spectral endoscopy of a 3-cm section of the esophagus (see methods) where the tumors were located.

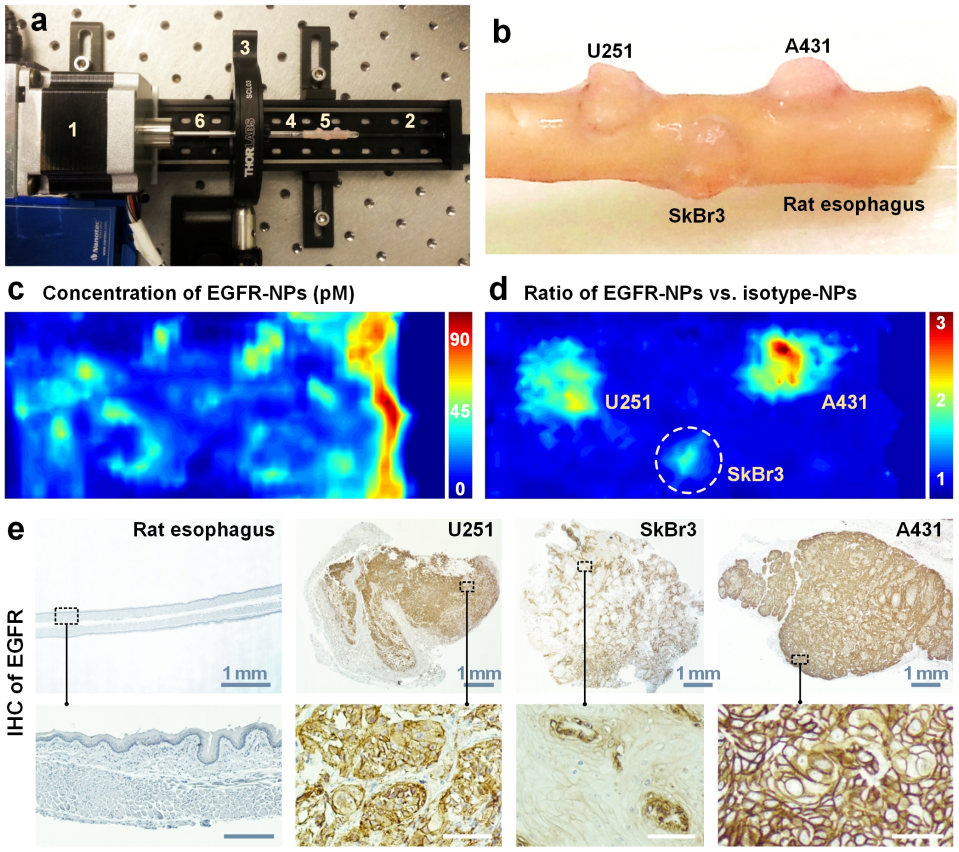

Fig. 3. *Ex vivo* imaging of the modified rat esophagus. (a) Photograph of the Raman endoscope. The numbered components are: 1. a stepper motor for rotational scanning; 2. a linear translation stage for axial scanning; 3. a holder for the glass tube; 4. the glass guide tube; 5. the rat esophagus; 6. the imaging probe. (b) Photograph of the esophageal cancer model with three different tumor xenografts. An image showing (c) the measured concentration of EGFR-NPs (in pM), which is ambiguous due to uneven delivery and nonspecific retention. These confounding effects are mitigated by imaging (d) the concentration ratio of EGFR-NPs vs. isotype-NPs. (e) Validation data: IHC for EGFR. The unlabeled scale bars in the bottom row of images represent 100 μm.

Figure 4(a) is a zoomed-in view of the surgically exposed cervical esophagus with 3 tumor implants. Figure 4(b) shows the reference spectrum of the SERS NPs, and Fig. 4(c) shows the background spectrum of esophagus tissues and raw (mixed) spectra acquired from NP-stained normal esophagus tissues and A431 tumor implants. Spectral demultiplexing reveals that the respective concentrations of the EGFR-NPs, HER2-NPs and isotype-NPs are 21.4 pM, 21.5 pM and 20.6 pM on the normal esophagus (blue spectrum) and 33.1 pM, 24.7 pM and 18.2 pM on the A431 tumor (red spectrum). The accuracy and linearity of the demultiplexing alogirithms used in this study have been demonstrated previously [24, 27].

Ratiometric images show the concentration ratios of EGFR-NPs vs. isotype-NPs (Fig. 4(d)) and HER2-NPs vs. isotype-NPs (Fig. 4(e)). These results demonstrate that multiplexed

#245684 Received 10 Jul 2015; revised 10 Aug 2015; accepted 24 Aug 2015; published 1 Sep 2015

ratiometric imaging of targeted vs. untargeted SERS NPs not only reveal the location of the receptor-positive tumors, but also quantify the EGFR and HER2 expression levels in agreement with flow-cytometry results (right-side plots in Figs. 4(d) and 4(e)). Note that while tumor cell suspensions yield specific-to-nonspecific binding ratios of up to two orders of magnitude in flow-cytometry experiments (Fig. 1), the molecular imaging of real tissues yields lower specific-to-nonspecific binding ratios due to less-ideal delivery of the NPs to cell-surface receptors as well as significantly higher nonspecific binding and retention effects, as discussed previously [24].

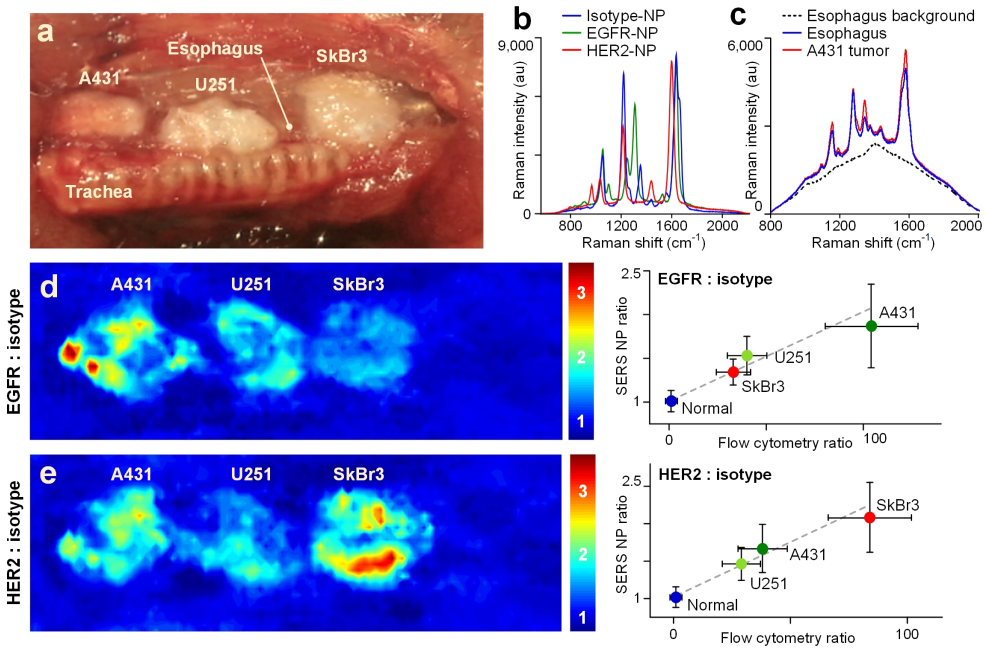

Fig. 4. *In vivo* endoscopic molecular imaging performed with multiplexed SERS NPs delivered via oral gavage. (a) Photograph of a surgically exposed rat esophagus implanted with three tumor xenografts. (b) Reference spectrum of the SERS NPs that were mixed together and topically applied into the rat esophagus in this study. (c) Background spectrum of esophagus tissues and raw (mixed) spectra acquired from NP-stained normal esophagus tissues and A431 tumor implants. (d and e) Images showing the concentration ratio of (d) EGFR-NPs vs. isotype-NPs and (e) HER2-NPs vs. isotype-NPs. The right-side plots show the correlation between the image-derived intensities from various tissue types (normal esophagus and three tumors) and the corresponding fluorescence ratio (targeted-NP vs. isotype-NP) from flow-cytometry experiments with the cell lines used to generate the various tumor xenografts (Fig. 1). All values in the figures are presented as mean ± standard deviation. $R > 0.95$.

4. Discussion

We have demonstrated an endoscopic imaging strategy for detecting and/or investigating gastrointestinal cancers that is based on the visualization of the molecular phenotype of tissues through the administration of molecularly targeted SERS NP contrast agents. Recently, SERS NPs have attracted much interest because of their high multiplexing capabilities, brightness, and minimal systemic uptake when applied to epithelial tissues including the gastrointestinal mucosa [25, 39]. In this study, we have developed and validated a miniature spectral endoscope to image SERS NPs topically applied within the rat esophagus for rapid tumor detection. The endoscope is able to comprehensively scan the entire lumen of the esophagus, via rotational pull-back of a spectral probe, with an imaging speed of 0.6 cm/min (10 spectra/sec). Although it requires more time than a localized point-detection method, the

#245684 Received 10 Jul 2015; revised 10 Aug 2015; accepted 24 Aug 2015; published 1 Sep 2015

strategy of comprehensively imaging the entire organ enables screening for molecular changes without prior knowledge about the location of potential lesions. Through imaging experiments with a rat esophageal tumor model, we have demonstrated that the miniature spectral endoscope can accurately locate and distinguish tumors by ratiometric quantification of targeted vs. untargeted SERS NPs, which enables the unambiguous visualization of biomarker-positive lesions. Furthermore, the ratiometric images agree with flow-cytometry and IHC validation data (Figs. 3 and 4).

SERS NPs are advantageous for multiplexed molecular imaging for a number of reasons. First, multiplexed SERS NPs may be excited at a single illumination wavelength (785 nm), ensuring that all NP reporters in a measurement are interrogated identically in terms of illumination intensity, area and depth. This ensures that ratiometric measurements are highly accurate and immune to wavelength-dependent tissue optical properties, which can plague fluorescence-based multiplexed imaging techniques in which disparate wavelength channels are often necessary. Second, the relatively large size of these NPs (~120 nm) allows them to remain at the surface of the esophagus lumen rather than diffusing into the tissue and being trapped, such that molecular image contrast between tumor and normal esophagus may be rapidly achieved (<15 min). Finally, the ratiometric quantification of targeted and control agents allows for the accurate identification of molecularly specific binding by eliminating nonspecific effects that are common in single-agent imaging, such as off-target binding, uneven agent delivery, and variations in tissue permeability and retention [24, 28–30].

Additional work is needed to further improve the spectral endoscopy technique. Brighter NPs would be of value to improve signal-to-noise ratios (SNR) and therefore, imaging speeds. While a few studies have shown the feasibility of detecting large multiplexed panels (5–10) of *untargeted* SERS NPs in animal or human tissues [14, 40], further work is needed to demonstrate the ability to quantify a large panel of tumor biomarkers with *targeted* SERS NPs such that tumors with heterogeneous biomarker expression patterns can be accurately identified. In addition, it will be interesting to test our endoscopy strategy with larger animal models, such as swine, which more closely resemble the human esophagus in terms of size and geometry. Since the ratiometric imaging of SERS NP mixtures is relatively insensitive to variations in working distance and tissue geometry [24, 29], the guide tube could be removed and a rotational Raman-imaging probe could be deployed through the instrument channel of a standard endoscope [17, 41]. These future studies will leverage our topical-delivery protocols and ratiometric-detection strategy to unambiguously visualize cell-surface biomarkers in tissues and may potentially improve the ability to detect and investigate esophageal cancer at the molecular level.

Acknowledgments

The authors acknowledge support from the NIH/NIBIB – R21 EB015016 (Liu), the Department of Biomedical Engineering at Stony Brook University (SUNY), the Department of Mechanical Engineering at the University of Washington, and the department of education GAANN fellowship program (SK).

#245684 Received 10 Jul 2015; revised 10 Aug 2015; accepted 24 Aug 2015; published 1 Sep 2015